

# Rendering Wireless Environments Useful for Gradient Estimators: A Zero-Order Stochastic Federated Learning Method

Elissa Mhanna and Mohamad Assaad

Laboratoire des Signaux et Systèmes  
Université Paris-Saclay, CNRS, CentraleSupélec  
91190 Gif-sur-Yvette, France

Email: {elissa.mhanna, mohamad.assaad}@centralesupelec.fr

**Abstract**—Federated learning (FL) is a novel approach to machine learning that allows multiple edge devices to collaboratively train a model without disclosing their raw data. However, several challenges hinder the practical implementation of this approach, especially when devices and the server communicate over wireless channels, as it suffers from communication and computation bottlenecks in this case. By utilizing a communication-efficient framework, we propose a novel zero-order (ZO) method with a one-point gradient estimator that harnesses the nature of the wireless communication channel without requiring the knowledge of the channel state coefficient. It is the first method that includes the wireless channel in the learning algorithm itself instead of wasting resources to analyze it and remove its impact. The two main difficulties of this work are that in FL, the objective function is usually not convex, which makes the extension of FL to ZO methods challenging, and that including the impact of wireless channels requires extra attention. However, we overcome these difficulties and comprehensively analyze the proposed zero-order federated learning (ZOFL) framework. We establish its convergence theoretically, and we prove a convergence rate of  $O(\frac{1}{\sqrt[3]{K}})$  in the nonconvex setting. We further demonstrate the potential of our algorithm with experimental results, taking into account independent and identically distributed (IID) and non-IID device data distributions.

## I. INTRODUCTION

ZO methods are a subfield of optimization that assume that first-order (FO) information or access to function gradients is unavailable. ZO optimization is based on estimating the gradient using function values queried at a certain number of points. The number of function queries depends on the assumptions of the problem. For example, in multi-point gradient estimates [1], [2], they construct the gradient by performing the difference of function values obtained at many random or predefined points. However, they assume that the stochastic setting stays the same during all these queries. For example, for functions  $\theta \mapsto f(\theta, S)$  subject to a stochastic variable  $S$ , two-point gradient estimates have the form,

$$g = d \frac{f(\theta + \gamma\Phi, S) - f(\theta - \gamma\Phi, S)}{2\gamma} \Phi,$$

with  $\theta \in \mathbb{R}^d$  the optimization variable,  $\gamma > 0$  a small value, and  $\Phi$  a random vector with a symmetric distribution. By contrast,

one-point estimates that use only one function value [3]–[5], principally obtained at a random point,

$$g = \frac{d}{\gamma} f(\theta + \gamma\Phi, S)\Phi,$$

assume that the settings are continuously changing during optimization. This is an important property as it resonates with many realistic applications, like when the optimization is performed in wireless environments or is based on previous simulation results. Recently, an appeal to ZO optimization is emerging in the machine-learning community, where optimizers are based on gradient methods. Examples include reinforcement learning [6], [7], generating contrastive explanations for black-box classification models [8], and effecting adversarial perturbations on such models [9], [10].

On the other hand, with the massive amounts of data generated or accessed by mobile devices, a growing research interest in both sectors of academia and industry [11] is focused on FL [12], [13], as it's a practical solution for training models on such data without the need to log them to a server. A lot of effort has been invested in developing first-order [12], [14], [15] and second-order [16], [17] methods to improve the efficacy of FL. These methods typically require access to the gradient or the Hessian of the local objective functions in their implementation to solve the optimization problem. However, using and exchanging such information raises many challenges, such as expensive communication and computation and privacy concerns [18].

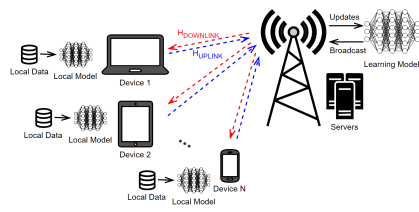


Fig. 1: Federated learning over wireless networks.

There is more interest recently in learning over wireless environments [19]–[24], with the increase of devices connected

to servers through cellular networks. In this paper, we are interested in this scenario illustrated in Fig. 1. Similarly to the aforementioned work, we are examining the case of analog communications between the devices and the server. However, it is a challenging problem as when the information is sent over the wireless channel, it becomes subject to a perturbation induced by the channel. This perturbation is not limited to additive noise, as noise is, in fact, due to thermal changes at the receiver. The channel acts as a filter for the transmitted signal [25], [26],

$$\hat{x} = Hx + n \quad (1)$$

where  $x$  and  $\hat{x} \in \mathbb{R}^d$  are the sent and received signals, respectively.  $H \in \mathbb{R}^{d \times d}$  is the channel matrix, and  $n \in \mathbb{R}^d$  is the additive noise, both of which are stochastic, constantly changing, and unknown. In general, all these entities are considered to have complex values. However, as we are interested in sending only real scalar values and we are not interested in decoding without error the sent information (but rather on using a perturbing on loss function), the phase shift introduced by the channel is considered as an additional perturbation in the channel model. Since our model is based on perturbing the loss function, considering only real values in the equation above is sufficient. We elaborate further on the channel modeling and why we can consider it real in Appendix A for the interested reader. In FL,  $x$  may denote the model or its gradients sent over the channel. To remove this impact, every channel element must be analyzed and removed to retrieve the sent information. This analysis is costly in computation and time resources. Thus, here our objective is to study FL in wireless environments without wasting resources.

Further, we are interested in exploring the potential of ZO optimization to deal with some of the difficulties demonstrated by FL. We then consider an FL setting where a central server coordinates with  $N$  edge devices to solve an optimization problem collaboratively. The data is private to every device and the exchanges between the server and the devices is restricted to the optimization parameters. To that end, let  $\mathcal{N} = \{1, \dots, N\}$  be the set of devices and  $\theta \in \mathbb{R}^d$  denote the global model. We define  $F_i : \mathbb{R}^d \rightarrow \mathbb{R}$  as the loss function associated with the local data stored on device  $i$ ,  $\forall i \in \mathcal{N}$ . The objective is to minimize the function  $F : \mathbb{R}^d \rightarrow \mathbb{R}$  that is composed of the said devices' loss functions, such that

$$\min_{\theta \in \mathbb{R}^d} F(\theta) := \sum_{i=1}^N F_i(\theta) \quad \text{with} \quad F_i(\theta) = \mathbb{E}_{S_i \sim D_i} f_i(\theta, S_i). \quad (2)$$

$S_i$  is an i.i.d. ergodic stochastic process following a local distribution  $D_i$ .  $S_i$  is used to model various stochastic perturbation, e.g. local data distribution among others. We further consider the case where the devices do not have access to their gradients for computational and communication restraints, and they must estimate this gradient by querying their model only once per update. They obtain a scalar value from this query (rather than a long vector as in the gradient), that they must send back to the server, which saves computation and communication

resources since only a scalar is computed instead of a long vector of gradient/model as in the standard gradient approach.

### A. Motivation for Our Work

**Communication Bottleneck.** In general, the main idea of FL is that the devices receive the model from the server, make use of their data to update the gradient, and then send back their gradients without ever disclosing their data. The server then updates the model using the collected and averaged gradients, and the process repeats. Since the gradients have the same dimension as the model, in every uplink step, there are  $Nd$  values that need to be uploaded, which forms the fundamental communication bottleneck in FL. To deal with this issue, some propose local multiple gradient descent steps to be done by the devices before sending their gradients back to the server to save communication resources [27], or allow partial device participation at every iteration [28], [29], or both [12]. Others propose lossy compression of the gradient before uploading it to the server. For example, all [30]–[32] suggest stochastic unbiased quantization approaches, where gradients are approximated with a finite set of discrete values for efficiency. [33] proposes the quantization of gradient differences of the current and previous iterations, allowing the update to incorporate new information, while [34] proposes the sparsification of this difference. Sparsification means that if a vector component is not large enough, it will not be transmitted.

**Channel Impact.** In FL over wireless channels, there is a problem with channel knowledge. When the devices upload their gradient  $g \in \mathbb{R}^d$  to the server, the server receives  $Hg + n$  as shown in equation (1). In [19] and [35] and all references within, they assume that they can remove the impact of the channel. However, as the channel matrix  $H$  coefficients follow a stochastic process and there are two unknown received entities, the channel  $H$  and the gradient, the knowledge of the gradient requires estimating the channel coefficients at each iteration of the FL. This requires computation resources, and more importantly, it requires resources to exchange control/reference signals between the devices and the server at each time/iteration to estimate the channel coefficients  $H$ . Alternatively, our work offers a much simpler approach. We do not waste resources trying to analyze the channel. We use the channel in the implementation itself. It is part of the learning. We harness it to construct our gradient estimate without the need to remove its impact, saving both computation and communication resources.

**Computation Demands.** Unlike standard methods that rely on the computational capabilities of participating devices, our approach is less demanding. Devices simply receive the global model, query it with their data, and send back the scalar loss, eliminating the need for "backward pass" computation. Only the "forward pass" is performed.

**Black-Box Optimization in FL.** One motivation for employing ZO methods is black-box problems [35] when gradient information cannot be acquired or is complicated to compute. For example, in hyperparameter tuning, gradients cannot be calculated, as there isn't an analytic relationship between the loss function and the hyperparameters [36].

### B. Challenges and Contribution

Addressing nonconvexity in FL is challenging. Our ZO method must handle nonconvexity, noise, and stochasticity efficiently, which can slow down convergence in gradient techniques. Additionally, the channel's introduction adds uncertainty and constraints on the number of communication exchanges. We need to ensure consistent and reliable performance, considering unknown probability distributions and fewer function evaluations. Unlike convex cases, nonconvex optimization does not allow easy quantification of optimization progress. Verifying gradient convergence becomes intricate due to biased gradient estimates. Moreover, unbounded variance in one-point estimates can lead to significant gradient deviations. These challenges involve technical and intuitive complexities we navigate.

In this work, we overcome these difficulties and propose a new communication-efficient algorithm in the nonconvex setting. This algorithm differs from the standard gradient method as it entails two reception-update steps instead of one, and it is not a simple extension of FO to ZO where the devices still have to upload their full model/gradient, as is the case in [35]. By limiting the exchange to scalar-valued updates, we counter the communication bottleneck, and we save up to a factor of  $O(d)$  per communication round, in comparison to standard methods, in terms of total exchanges of variables between the devices and the server, saving a lot of execution time. We harness the nature of autocorrelated channels for truly "blind" reception of the data. We prove the convergence theoretically with a one-point estimate and provide experimental evidence. An important distinction worth noting is that standard ZO methods establish convergence by focusing on the expected convergence of the exact gradient. In contrast to prior research, our approach goes further in the proof. We demonstrate the convergence of the exact gradient itself almost surely, not solely its expected value. The key element in this proof is employing Doob's martingale inequality to constrain the stochastic error resulting from the estimated gradient. We finally extend the analysis to non-symmetrical channel models, i.e., channels without zero-mean, and thus provide a practical algorithm for general settings.

## II. ALGORITHM

This section illustrates our proposed zero-order stochastic federated learning algorithm with a new gradient estimator (ZOFL).

### A. The 1P-ZOFL Algorithm

We consider an intermediary wireless environment between the server and each device  $i$  for  $i \in \mathcal{N}$  as shown in Fig. 1. Wireless channels introduce a stochastic scaling on the sent signal as elaborated in equation (1). As we only send a scalar value over the channel at a time, our channel has only one scalar coefficient in addition to a scalar noise. Channel coefficients are usually autocorrelated from one timeslot to the next. Let  $h_{i,k}$  denote the channel scaling affecting the sent signal from device  $i$  to the server at timeslot  $k$ , independent from all other devices' channels. We assume  $h_{i,k}$  to be a zero-mean random

---

### Algorithm 1 The 1P-ZOFL Algorithm

---

**Input:** Initial model  $\theta_0 \in \mathbb{R}^d$ , the initial step-sizes  $\alpha_0$  and  $\gamma_0$ , and the channels' standard deviation  $\sigma_h$

- 1: **for**  $k = 0, 2, 4, \dots$  **do**
- 2:     The server receives  $\sum_{j=1}^N \frac{h_{j,k}}{\sigma_h^2} + n_{j,k}$
- 3:     The server broadcasts  $\theta_k + \gamma_k \Phi_k \sum_{j=1}^N \left( \frac{h_{j,k}}{\sigma_h^2} + n_{j,k} \right)$  to all devices
- 4:     The server receives  $\sum_{i=1}^N h_{i,k+1} \tilde{f}_i \left( \theta_k + \gamma_k \Phi_k \sum_{j=1}^N \left( \frac{h_{j,k}}{\sigma_h^2} + n_{j,k} \right), S_{i,k+1} \right) + n_{i,k+1}$
- 5:     The server multiplies the received scalar sum by  $\Phi_k$  to assemble  $g_k$  given in (3)
- 6:     The server updates  $\theta_{k+1} = \theta_k - \alpha_k g_k$
- 7: **end for**

---

variable with standard deviation  $\sigma_h$ ,  $\forall i \in \mathcal{N}, \forall k \in \mathbb{N}^+$ , and  $n_{i,k}$  an additive noise on the transmitted signal. Assuming that the channel is time-correlated for two consecutive iterations  $k$  and  $k+1$ , such that the autocovariance is  $\mathbb{E}[h_{i,k}h_{i,k+1}] = K_{hh}$ ,  $\forall i \in \mathcal{N}, \forall k \in \mathbb{N}^+$ , we present our learning method in Algorithm 1:

The devices must carry out two communication steps. In the first, every device sends the value  $\frac{1}{\sigma_h^2}$  to the server. According to equation (1), the server receives  $\frac{h_{j,k}}{\sigma_h^2} + n_{j,k}$  from every device  $j$ . Hence, it receives the sum in step 2. Afterward, the server uses the values received to adjust the model and broadcasts it to the devices. When device  $i$  receives the model, it receives  $h_{i,k+1}^{DL} [\theta_k + \gamma_k \Phi_k \sum_{j=1}^N (\frac{h_{j,k}}{\sigma_h^2} + n_{j,k})] + n_{i,k+1}^{DL}$ , and to simplify notation, we let the stochastic vector  $[h_{i,k+1}^{DL}, n_{i,k+1}^{DL}]$  be included within the big vector  $S_{i,k+1}$  of stochastic perturbations. Device  $i$  then queries this received model to obtain the stochastic loss  $f_i$ . Then the devices send  $f$  to the server in the second communication step, and according to equation (1), the server receives the quantity indicated in step 4. Finally, the server assembles the gradient estimate and is able to update  $\theta$  according to step 7. All transmissions are subject to channel scaling and additive noise. We designate them by  $h$  and  $n$  in the device-to-server transmission. In the server-to-devices one, we designate them by  $S$ . We let  $\tilde{f}_i = \frac{f_i}{\sigma_h^2}$  be the normalized loss function and define  $\alpha_k$  and  $\gamma_k$  as two step-sizes and  $\Phi_k \in \mathbb{R}^d$  as a perturbation vector generated by the server that has the same dimension as that of the model.

We emphasize here that  $g_k$  (in step 6) is the gradient estimate in this case, and one can see that the impact of the channel is included in the gradient estimate and hence in the learning. The major advantage of this algorithm is that each device sends only two scalar values. This is stark improvement in communication efficiency over standard FL algorithms that require each device to send back the whole model or local gradient of dimension  $d$ . In effect, it is resource draining and can be unrealistic to assume it is possible.

## B. The Estimated Gradient

We provide here analysis of our ZO gradient estimate. We propose the one-point estimate:

$$g_k = \Phi_k \sum_{i=1}^N \left[ h_{i,k+1} \tilde{f}_i \left( \theta'_k, S_{i,k+1} \right) + n_{i,k+1} \right], \quad (3)$$

where  $\theta'_k = \theta_k + \gamma_k \Phi_k \sum_{j=1}^N \left( \frac{h_{j,k}}{\sigma_h^2} + n_{j,k} \right)$ . The values  $h_{i,k}$ ,  $h_{i,k+1}$ , and the noise remain unknown. This saves computation complexity and is very communication efficient as it transcends the need to send pilot signals to estimate the channel continuously.

We next consider the following assumptions on the additive noise, the perturbation vector, and the local loss functions.

*Assumption 1:*  $n_{i,k}$  is assumed to be a zero-mean uncorrelated noise with bounded variance, meaning  $E(n_{i,k}) = 0$  and  $E(n_{i,k}^2) = \sigma_n^2 < \infty$ ,  $\forall i \in \mathcal{N}$ ,  $\forall k \in \mathbb{N}^+$ . For any timeslot  $k$ ,  $E(n_{i,k} n_{j,k}) = 0$  if  $i \neq j$ . For any device  $i$ ,  $E(n_{i,k} n_{i,k'}) = 0$  if  $k \neq k'$ .

*Assumption 2:* Let  $\Phi_k = (\phi_k^1, \phi_k^2, \dots, \phi_k^d)^T$ . At each iteration  $k$ , the server generates its  $\Phi_k$  vector independently from other iterations. In addition, the elements of  $\Phi_k$  are assumed i.i.d with  $E(\phi_k^{d_1} \phi_k^{d_2}) = 0$  for  $d_1 \neq d_2$  and there exists  $\alpha_2 > 0$  such that  $E(\phi_k^{d_j})^2 = \alpha_2$ ,  $\forall d_j$ ,  $\forall k$ . We further assume there exists a constant  $\alpha_3 > 0$  where  $\|\Phi_k\| \leq \alpha_3$ ,  $\forall k$ .

*Example 1:* An example of a perturbation vector satisfying Assumption 2, is picking every dimension of  $\Phi_k$  from  $\{-\frac{1}{\sqrt{d}}, \frac{1}{\sqrt{d}}\}$  with equal probability. Then,  $\alpha_2 = \frac{1}{d}$  and  $\alpha_3 = 1$ .

*Assumption 3:* All loss functions  $\theta \mapsto f_i(\theta, S_i)$  are Lipschitz continuous with Lipschitz constant  $L_{S_i}$ ,  $|f_i(\theta, S_i) - f_i(\theta', S_i)| \leq L_{S_i} \|\theta - \theta'\|$ ,  $\forall i \in \mathcal{N}$ . In addition,  $\mathbb{E}_{S_i} f_i(\theta, S_i) < \infty$ ,  $\forall i \in \mathcal{N}$ .

Let  $\mathcal{H}_k = \{\theta_0, S_0, \theta_1, S_1, \dots, \theta_k, S_k\}$  denote the history sequence, then the following two lemmas characterize our gradient estimate.

*Lemma 1:* Let Assumptions 1 and 2 be satisfied and define the scalar value  $c_1 = \alpha_2 \frac{K_{h,h}}{\sigma_h^4}$ , then the gradient estimator is biased w.r.t. the objective function's exact gradient  $\nabla F(\theta)$ . Concretely,  $\mathbb{E}[g_k | \mathcal{H}_k] = c_1 \gamma_k (\nabla F(\theta_k) + b_k)$   $\forall k \in \mathbb{N}^+$ , where  $b_k$  is the bias term.

Proof: Refer to Appendix B-A.

*Lemma 2:* Let Assumptions 1-3 and the inequality  $\|\theta_k\| < \infty$  hold almost surely. There exist a bounded constant  $c_2 > 0$ , such that  $\mathbb{E}[\|g_k\|^2 | \mathcal{H}_k] \leq c_2$  almost surely.

Proof: Refer to Appendix B-B.

## III. CONVERGENCE ANALYSIS

We begin by assuming that a global minimizer  $\theta^* \in \mathbb{R}^d$  exists such that  $\min_{\theta \in \mathbb{R}^d} F(\theta) = F(\theta^*) > -\infty$  and  $\nabla F(\theta^*) = 0$ .

*Assumption 4:* We assume the existence and the continuity of  $\nabla F_i(\theta)$  and  $\nabla^2 F_i(\theta)$ , and that there exists a constant  $\alpha_1 > 0$  such that  $\|\nabla^2 F_i(\theta)\|_2 \leq \alpha_1$ ,  $\forall i \in \mathcal{N}$ .

*Lemma 3:* By Assumption 4, we know that the objective function  $\theta \mapsto F(\theta)$  is  $L$ -smooth for some positive constant  $L$ ,  $\|\nabla F(\theta) - \nabla F(\theta')\| \leq L \|\theta - \theta'\|$ ,  $\forall \theta, \theta' \in \mathbb{R}^d$ , or equivalently,  $F(\theta) \leq F(\theta') + \langle \nabla F(\theta'), \theta - \theta' \rangle + \frac{L}{2} \|\theta - \theta'\|^2$ .

*Lemma 4:* By Assumptions 1, 2, and 4, we can find a scalar value  $c_3 > 0$  such that  $\|b_k\| \leq c_3 \gamma_k$ .

Proof: Refer to Appendix B-C.

### A. IP-ZOFL convergence

In Lemma 1, we see that in expectation, our estimator deviates from the gradient direction by the bias term. To provide that this term does not grow larger and preferably grows smaller as the algorithm evolves, we impose that  $\gamma_k$  vanishes. Additionally, to ensure that the expected norm squared of the estimator, as shown in Lemma 2, does not accumulate residual constant terms, we impose that the step size  $\alpha_k$  vanishes. The series properties in the following assumption come from the recursive analysis of the algorithm.

*Assumption 5:* Both the step sizes  $\alpha_k$  and  $\gamma_k$  vanish to zero as  $k \rightarrow \infty$  and the following series composed of them satisfy the convergence assumptions  $\sum_{k=0}^{\infty} \alpha_k \gamma_k = \infty$ ,  $\sum_{k=0}^{\infty} \alpha_k \gamma_k^3 < \infty$ , and  $\sum_{k=0}^{\infty} \alpha_k^2 < \infty$ .

*Example 2:* To satisfy Assumption 5, we consider the following form of the step sizes,  $\alpha_k = \alpha_0(1+k)^{-v_1}$  and  $\gamma_k = \gamma_0(1+k)^{-v_2}$  with  $v_1, v_2 > 0$ . Then, it is sufficient to find  $v_1$  and  $v_2$  such that  $0 < v_1 + v_2 \leq 1$ ,  $v_1 + 3v_2 > 1$ , and  $v_1 > 0.5$ .

We next define the stochastic error  $e_k$  as the difference between the value of a single realization of  $g_k$  and its conditional expectation given the history sequence, i.e.,  $e_k = g_k - \mathbb{E}[g_k | \mathcal{H}_k]$ .

The study of this noise and how it evolves is essential for the analysis of the algorithm as it gives access to the exact gradient when examining the algorithm's convergence behavior and permits us to prove that, in fact, the exact gradient converges to zero and not just the expectation of the exact gradient. This is a stronger convergence property, and it has not been done before in ZO nonconvex optimization to the best of our knowledge. The trick is to show that  $e_k$  is a martingale difference sequence and to apply Doob's martingale inequality to derive the following lemma.

*Lemma 5:* If all Assumptions 1-5 hold and  $\|\theta_k\| < \infty$  almost surely, then for any constant  $\nu > 0$ , we have  $\mathbb{P}(\lim_{K \rightarrow \infty} \sup_{K' \geq K} \|\sum_{k=K}^{K'} \alpha_k e_k\| \geq \nu) = 0$ .

Proof: Refer to Appendix C-A.

The smoothness inequality allows for the first main result, leading to the second in the following theorem.

*Theorem 1:* When Assumptions 1-5 hold, we have  $\sum_k \alpha_k \gamma_k \|\nabla F(\theta_k)\|^2 < +\infty$  and  $\lim_{k \rightarrow \infty} \|\nabla F(\theta_k)\| = 0$  almost surely, meaning that the algorithm converges.

Proof: Refer to Appendix C-B.

Proof sketch: We substitute the algorithm's updates in the second inequality of Lemma 3 and replace the estimate by its expectation plus the stochastic error. We then perform a recursive addition over the iterations  $k > 0$ . With Lemma 5, the conditions on the step sizes, and the upper bound estimate's squared norm, we are able to find an upper bound on  $\sum_k \alpha_k \gamma_k \|\nabla F(\theta_k)\|^2$  when  $k$  grows to  $\infty$ . The next step is to consider the hypothesis  $\lim_{k \rightarrow \infty} \sup \|\nabla F(\theta_k)\| \geq \rho$ , for  $\rho > 0$ , and prove that it contradicts with the first result.

Define  $\delta_k = F(\theta_k) - F(\theta^*)$ . We next find an upper bound on the convergence rate of Algorithm 1.

*Theorem 2:* Consider in addition to the assumptions in Theorem 1, that the step sizes are those of Example 2 with  $v_3 = v_1 + v_2 < 1$ . Then, we can write

$$\frac{\sum_k \alpha_k \gamma_k \mathbb{E}[\|\nabla F(\theta_k)\|^2]}{\sum_k \alpha_k \gamma_k} \leq \frac{A(1-v_3)}{(K+2)^{1-v_3} - 1}. \quad (4)$$

with  $A = \frac{2\delta_0}{c_1\alpha_0\gamma_0} + c_3^2\gamma_0^2\left(\frac{v_1+3v_2}{v_1+3v_2-1}\right) + \frac{Lc_2\alpha_0}{c_1\gamma_0}\left(\frac{2v_1}{2v_1-1}\right)$ .

Proof: Refer to Appendix C-C.

In Theorem 2, we see that the optimal choice of the exponents for the time-varying component  $O(\frac{1}{K^{1-v_1-v_2}})$ , is  $v_1 = \frac{1}{2}$  and  $v_2 = \frac{1}{6}$  for a rate of  $O(\frac{1}{\sqrt[3]{K}})$ . However, to prevent the constant component from growing too large, it is recommended to choose slightly larger exponents of  $v_1 = \frac{1}{2} + \frac{\epsilon}{2}$  and  $v_2 = \frac{1}{6} + \frac{\epsilon}{2}$ , where  $\epsilon$  is a small strictly positive value. This will result in a rate of  $O(\frac{1}{K^{\frac{1}{3}-\epsilon}})$ .

### B. Non-Symmetrical Channels Case

Assuming a non-symmetrical channel model with  $\mathbb{E}[h_{i,k}] = \mu_h$  and  $\sigma_h^2 = \mathbb{E}[h_{i,k}^2] - \mu_h^2$ ,  $\forall i, \forall k$ , we provide how our gradient estimates and algorithms can be adjusted in Appendix D to account for this case. In fact, non-symmetrical channel models (e.g., Rician) offer a simplification of both analysis and implementation in comparison to symmetrical models (e.g., Rayleigh), as the non-zero mean no longer cancels out the gradient, and the design is further independent of the autocorrelation of the channels.

## IV. EXPERIMENTAL RESULTS

For the experimental results, we test our algorithms in nonconvex binary image classification problems, and we compare them against the original FL algorithm FedAvg [12] with exact gradient and one local update per round. However, we do not consider the effect of the channel or any noise/stochasticity for the FedAvg algorithm. All experiments are done for 100 devices and data batches of 10 images per user per round. Every communication round in the graphs include all steps 2 through 7 for Algorithm 1.

We classify photos of the two digits “0” and “1” from the MNIST dataset [37] using a nonconvex logistic regression model with a regularization parameter of 0.001. All images are divided equally among the devices and are considered to be preprocessed by being compressed to have dimension  $d = 10$  using a lossy autoencoder. We run our code on 50 simulations with different random model initializations testing the accuracy in every iteration against an independent test set. The graphs in Fig. 2 are averaged over all these simulations. For the non-IID data distribution, we first sort the images according to their labels and then divide them among the devices.  $\Phi_k$  is generated according to Example 1. All channels are generated using the normal distribution with autocovariance  $K_{hh} = \frac{1}{2}$ . The noise is Gaussian with 0 mean and variance  $\sigma_n^2 = \frac{1}{4}$ . The step size for FedAvg is taken as  $\eta = 0.15$ . For 1P-ZOFL,  $\alpha_k = 0.5(1+k)^{-0.51}$  and  $\gamma_k = 2.5(1+k)^{-0.18}$ . Our algorithm performs consistently well with all the different

random variations influencing every simulation in line with our theoretical results. Considering non-IID data distribution seems to be better impacted by our ZO algorithm slightly at the beginning without a major effect on the final result.

In Fig. 3, we test our algorithm with different noise variance  $\sigma_n^2$  and notice that while the algorithm is slowed slightly at the beginning, it does not affect the convergence. When  $\sigma_n^2 = 2.25$ , we change  $\alpha_0 = 0.1$  and  $\gamma_0 = 0.8$ . When  $\sigma_n^2 = 10.0489$ ,  $\alpha_0 = 0.07$  and  $\gamma_0 = 0.3$ . We provide all other details alongside a discussion of our algorithm’s performance in relation to the noise variance in Appendix E.

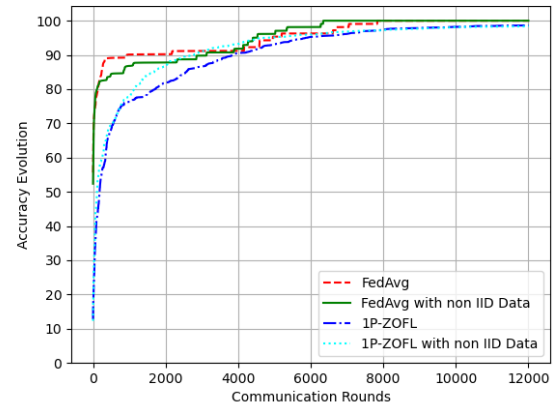


Fig. 2: Accuracy evolution of 1P-ZOFL vs. FedAvg for IID data and non-IID distribution.

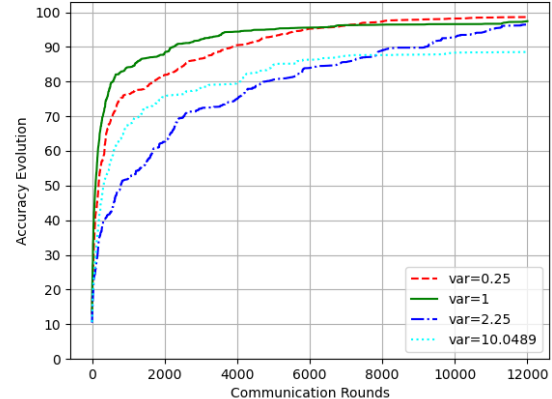


Fig. 3: Accuracy evolution of 1P-ZOFL for  $\sigma_n^2 = \{0.25, 1, 2.25, 10.0489\}$ .

## V. CONCLUSION

This work considers a learning problem over wireless channels and proposes a new zero-order federated learning method with a one-point gradient estimator. We limit the communication to scalar-valued feedback from the devices and incorporate the wireless channel in the learning algorithm. We provide theoretical and experimental evidence for convergence and find an upper bound on the convergence rate.

## REFERENCES

[1] J. C. Duchi, M. I. Jordan, M. J. Wainwright, and A. Wibisono, “Optimal rates for zero-order convex optimization: The power of two function evaluations,” *IEEE Transactions on Information Theory*, vol. 61, no. 5, pp. 2788–2806, 2015.

[2] A. Agarwal, O. Dekel, and L. Xiao, “Optimal algorithms for online convex optimization with multi-point bandit feedback,” in *COLT*, 2010.

[3] A. Flaxman, A. T. Kalai, and H. B. McMahan, “Online convex optimization in the bandit setting: gradient descent without a gradient,” *CoRR*, vol. cs.LG/0408007, 2004. [Online]. Available: <http://arxiv.org/abs/cs.LG/0408007>

[4] W. Li and M. Assaad, “Distributed stochastic optimization in networks with low informational exchange,” *IEEE Transactions on Information Theory*, vol. 67, no. 5, pp. 2989–3008, 2021.

[5] E. Mhanna and M. Assaad, “Zero-order one-point estimate with distributed stochastic gradient-tracking technique,” 2022. [Online]. Available: <https://arxiv.org/abs/2210.05618>

[6] A. Vemula, W. Sun, and J. Bagnell, “Contrasting exploration in parameter and action space: A zeroth-order optimization perspective,” in *Proceedings of the Twenty-Second International Conference on Artificial Intelligence and Statistics*, vol. 89. PMLR, 16–18 Apr 2019, pp. 2926–2935.

[7] D. Malik, A. Pananjady, K. Bhatia, K. Khamaru, P. Bartlett, and M. Wainwright, “Derivative-free methods for policy optimization: Guarantees for linear quadratic systems,” in *Proceedings of the Twenty-Second International Conference on Artificial Intelligence and Statistics*, vol. 89. PMLR, 16–18 Apr 2019, pp. 2916–2925.

[8] A. Dhurandhar, T. Pedapati, A. Balakrishnan, P.-Y. Chen, K. Shannugam, and R. Puri, “Model agnostic contrastive explanations for structured data,” 2019.

[9] A. Ilyas, L. Engstrom, A. Athalye, and J. Lin, “Black-box adversarial attacks with limited queries and information,” in *Proceedings of the 35th International Conference on Machine Learning*, vol. 80. PMLR, 10–15 Jul 2018, pp. 2137–2146.

[10] X. Chen, S. Liu, K. Xu, X. Li, X. Lin, M. Hong, and D. Cox, “Zo-adamm: Zeroth-order adaptive momentum method for black-box optimization,” in *Advances in Neural Information Processing Systems*, vol. 32. Curran Associates, Inc., 2019.

[11] K. Bonawitz, H. Eichner, W. Grieskamp, D. Huba, A. Ingerman, V. Ivanov, C. Kiddon, J. Konečný, S. Mazzocchi, B. McMahan, T. Van Overveldt, D. Petrou, D. Ramage, and J. Roselander, “Towards federated learning at scale: System design,” in *Proceedings of Machine Learning and Systems*, vol. 1, 2019, pp. 374–388.

[12] B. McMahan, E. Moore, D. Ramage, S. Hampson, and B. A. y. Arcas, “Communication-Efficient Learning of Deep Networks from Decentralized Data,” in *Proceedings of the 20th International Conference on Artificial Intelligence and Statistics*, vol. 54. PMLR, 20–22 Apr 2017, pp. 1273–1282.

[13] P. Kairouz, H. B. McMahan, B. Avent, A. Bellet, M. Bennis, A. N. Bhagoji, K. Bonawitz, Z. Charles, G. Cormode, R. Cummings, R. G. L. D’Oliveira, H. Eichner, S. El Rouayheb, D. Evans, J. Gardner, Z. Garrett, A. Gascón, B. Ghazi, P. B. Gibbons, M. Gruteser, Z. Harchaoui, C. He, L. He, Z. Huo, B. Hutchinson, J. Hsu, M. Jaggi, T. Javidi, G. Joshi, M. Khodak, J. Konečný, A. Korolova, F. Koushanfar, S. Koyejo, T. Lepoint, Y. Liu, P. Mittal, M. Mohri, R. Nock, A. Özgür, R. Pagh, H. Qi, D. Ramage, R. Raskar, M. Raykova, D. Song, W. Song, S. U. Stich, Z. Sun, A. Theertha Suresh, F. Tramèr, P. Vepakomma, J. Wang, L. Xiong, Z. Xu, Q. Yang, F. X. Yu, H. Yu, and S. Zhao, 2021.

[14] X. Zhang, M. Hong, S. Dhopde, W. Yin, and Y. Liu, “Fedpd: A federated learning framework with adaptivity to non-iid data,” *IEEE Transactions on Signal Processing*, vol. 69, pp. 6055–6070, 2021.

[15] J. Wang, Q. Liu, H. Liang, G. Joshi, and H. V. Poor, “A novel framework for the analysis and design of heterogeneous federated learning,” *IEEE Transactions on Signal Processing*, vol. 69, pp. 5234–5249, 2021.

[16] A. Elgabli, C. B. Issaid, A. S. Bedi, K. Rajawat, M. Bennis, and V. Aggarwal, “FedNew: A communication-efficient and privacy-preserving Newton-type method for federated learning,” in *Proceedings of the 39th International Conference on Machine Learning*, vol. 162. PMLR, 17–23 Jul 2022, pp. 5861–5877.

[17] T. Li, A. K. Sahu, M. Zaheer, M. Sanjabi, A. Talwalkar, and V. Smithy, “Feddane: A federated newton-type method,” in *2019 53rd Asilomar Conference on Signals, Systems, and Computers*, 2019, pp. 1227–1231.

[18] T. Li, A. K. Sahu, A. Talwalkar, and V. Smithy, “Federated learning: Challenges, methods, and future directions,” *IEEE Signal Processing Magazine*, vol. 37, no. 3, pp. 50–60, 2020.

[19] K. Yang, T. Jiang, Y. Shi, and Z. Ding, “Federated learning via over-the-air computation,” *IEEE Transactions on Wireless Communications*, vol. 19, no. 3, pp. 2022–2035, 2020.

[20] M. M. Amiri and D. Gündüz, “Federated learning over wireless fading channels,” *IEEE Transactions on Wireless Communications*, vol. 19, no. 5, pp. 3546–3557, 2020.

[21] T. Sery and K. Cohen, “On analog gradient descent learning over multiple access fading channels,” *IEEE Transactions on Signal Processing*, vol. 68, pp. 2897–2911, 2020.

[22] H. Guo, A. Liu, and V. K. N. Lau, “Analog gradient aggregation for federated learning over wireless networks: Customized design and convergence analysis,” *IEEE Internet of Things Journal*, vol. 8, no. 1, pp. 197–210, 2021.

[23] T. Sery, N. Shlezinger, K. Cohen, and Y. C. Eldar, “Over-the-air federated learning from heterogeneous data,” *IEEE Transactions on Signal Processing*, vol. 69, pp. 3796–3811, 2021.

[24] Y. Sun, S. Zhou, Z. Niu, and D. Gündüz, “Dynamic scheduling for over-the-air federated edge learning with energy constraints,” *IEEE Journal on Selected Areas in Communications*, vol. 40, no. 1, pp. 227–242, 2022.

[25] D. Tse and P. Viswanath, *Fundamentals of Wireless Communication*. Cambridge University Press, 2005.

[26] E. Björnson and L. Sanguinetti, “Making cell-free massive mimo competitive with mmse processing and centralized implementation,” *IEEE Transactions on Wireless Communications*, vol. 19, no. 1, pp. 77–90, 2020.

[27] A. Khaled, K. Mishchenko, and P. Richtarik, “Tighter theory for local sgd on identical and heterogeneous data,” in *Proceedings of the Twenty-Third International Conference on Artificial Intelligence and Statistics*, vol. 108. PMLR, 26–28 Aug 2020, pp. 4519–4529.

[28] T. Chen, G. Giannakis, T. Sun, and W. Yin, “Lag: Lazily aggregated gradient for communication-efficient distributed learning,” in *Advances in Neural Information Processing Systems*, vol. 31. Curran Associates, Inc., 2018. [Online]. Available: <https://proceedings.neurips.cc/paper/2018/file/feccce9f1643651799ede2740927317a-Paper.pdf>

[29] M. M. Amiri, D. Gündüz, S. R. Kulkarni, and H. V. Poor, “Convergence of update aware device scheduling for federated learning at the wireless edge,” *IEEE Transactions on Wireless Communications*, vol. 20, no. 6, pp. 3643–3658, 2021.

[30] J. Konečný, H. B. McMahan, F. X. Yu, P. Richtárik, A. T. Suresh, and D. Bacon, “Federated learning: Strategies for improving communication efficiency,” 2016. [Online]. Available: <https://arxiv.org/abs/1610.05492>

[31] S. Khirirat, H. R. Feyzmahdavian, and M. Johansson, “Distributed learning with compressed gradients,” 2018. [Online]. Available: <https://arxiv.org/abs/1806.06573>

[32] A. Elgabli, J. Park, A. S. Bedi, M. Bennis, and V. Aggarwal, “Q-gadmm: Quantized group admm for communication efficient decentralized machine learning,” in *ICASSP 2020 - 2020 IEEE International Conference on Acoustics, Speech and Signal Processing (ICASSP)*, 2020, pp. 8876–8880.

[33] K. Mishchenko, E. Gorbunov, M. Takáč, and P. Richtárik, “Distributed learning with compressed gradient differences,” 2019. [Online]. Available: <https://arxiv.org/abs/1901.09269>

[34] Y. Chen, R. S. Blum, M. Takáč, and B. M. Sadler, “Distributed learning with sparsified gradient differences,” *IEEE Journal of Selected Topics in Signal Processing*, vol. 16, no. 3, pp. 585–600, 2022.

[35] W. Fang, Z. Yu, Y. Jiang, Y. Shi, C. N. Jones, and Y. Zhou, “Communication-efficient stochastic zeroth-order optimization for federated learning,” *IEEE Transactions on Signal Processing*, vol. 70, pp. 5058–5073, 2022.

[36] Z. Dai, B. K. H. Low, and P. Jaillet, “Federated bayesian optimization via thompson sampling,” in *Advances in Neural Information Processing Systems*, vol. 33. Curran Associates, Inc., 2020, pp. 9687–9699.

[37] Y. LeCun and C. Cortes, “The MNIST database of handwritten digits,” 2005.

[38] J. L. Doob, “Stochastic processes,” 1953.

## APPENDIX A ON THE CHANNEL MODEL

As described in Section 2.2 of Chapter 2 of [25] and considering a double-sideband suppressed carrier amplitude modulation (DSB-SC) instead of quadrature amplitude modulation (QAM):

Having a baseband signal  $x$ , to send it over the channel, we modulate (multiply) it by  $\sqrt{2} \cos 2\pi f_c t$  where  $f_c$  is the carrier frequency and  $t$  is the time index.

When sent over the channel, the transmitted signal  $x$  undergoes perturbation and thus the received signal becomes:

$$z = \sqrt{2} \sum_i a_i x \cos(2\pi f_c t + \varphi_i(t)) + w(t), \quad (5)$$

where  $a_i$  is the amplitude attenuation of path  $i$  and  $\varphi_i(t) = 2\pi f_l t + \varphi_l$  is the phase shift incurred by Doppler frequency shift  $f_l$  and/or any time delay  $\varphi_l$ .  $w(t)$  is an additive noise.

By developing the cosine term in  $z$ , we obtain

$$\begin{aligned} z = & x \sqrt{2} \underbrace{\sum_i a_i \cos(\varphi_i(t)) \cos(2\pi f_c t)}_{\text{in-phase component, } I(t)} \\ & - x \sqrt{2} \underbrace{\sum_i a_i \sin(\varphi_i(t)) \sin(2\pi f_c t)}_{\text{quadrature component, } Q(t)} + w(t), \end{aligned} \quad (6)$$

From Section 2.4.2 of [25]: According to the central limit theorem, if there is a large number of channel paths, the in-phase and quadrature components of the received signal, which are not correlated with each other, will exhibit distributions that resemble the normal (Gaussian) distribution. Specifically, each component will have an average value of zero and a variance of  $\Sigma/2$ , which is equivalent to  $\sigma^2$ . The magnitude of the perturbation  $\sqrt{I(t)^2 + Q(t)^2}$  thus becomes Rayleigh distributed. This is the Rayleigh fading model. In addition, when the line-of-sight path is large and has a known magnitude, the probabilistic model becomes a Rician fading.

Furthermore, as  $I(t)$  and  $Q(t)$  are orthogonal, an equivalent complex channel model  $\hat{h}(t) = I(t) + jQ(t) = a(t)e^{-j\varphi(t)}$  can be derived. Since the carrier frequency  $f_c$  is not involved in  $\hat{h}(t)$ , this representation is valid at baseband level. Thus, the complex channel model is usually used to represent the received signal  $\hat{h}(t)x + n(t)$  at baseband with  $\hat{h}(t)$  a complex entity.

Continuing from (6), to demodulate  $z$  and obtain the baseband received signal  $y$ ,  $z$  is first multiplied by  $\sqrt{2} \cos 2\pi f_c t$  then the result goes through a low pass filter.

$$\begin{aligned} & z \sqrt{2} \cos(2\pi f_c t) \\ &= 2x \sum_i a_i \cos(\varphi_i(t)) \cos^2(2\pi f_c t) \\ & \quad - 2x \sum_i a_i \sin(\varphi_i(t)) \sin(2\pi f_c t) \cos(2\pi f_c t) \\ & \quad + \sqrt{2} w(t) \cos(2\pi f_c t) \end{aligned}$$

$$\begin{aligned} &= x \sum_i a_i \cos(\varphi_i(t)) (1 + \cos(4\pi f_c t)) \\ & \quad - x \sum_i a_i \sin(\varphi_i(t)) \sin(4\pi f_c t) + \sqrt{2} w(t) \cos(2\pi f_c t) \end{aligned} \quad (7)$$

After the low pass filter, we obtain the received baseband signal

$$\begin{aligned} y &= x \sum_i a_i \cos(\varphi_i(t)) + n(t) \\ &= \Re[\hat{h}(t)]x + n(t) \\ &= h(t)x + n(t) \end{aligned} \quad (8)$$

where  $n(t)$  is the baseband equivalent noise with a zero-mean Gaussian distribution and IID components (Section 2.2.4 of [25]) and  $\Re[\hat{h}(t)] = I(t)$  is the real part of the channel.

As we are interested to send real values over the wireless channel in this paper, one can easily see how equation (8) is valid to use with a real channel  $h = \Re[\hat{h}]$  following a Gaussian distribution with zero mean and variance equal to  $\sigma^2$ .

## APPENDIX B ON THE ESTIMATED GRADIENT

### A. Proof of Lemma 1: Biased Estimator

Let  $g_k$  have the form in (3), then the conditional expectation given  $\mathcal{H}_k$  can be written as

$$\begin{aligned} & \mathbb{E}[g_k | \mathcal{H}_k] \\ &= \mathbb{E}\left[\Phi_k \sum_{i=1}^N \left(h_{i,k+1} \tilde{f}_i(\theta'_k, S_{i,k+1}) + n_{i,k+1}\right) \middle| \mathcal{H}_k\right] \\ &\stackrel{(a)}{=} \mathbb{E}\left[\Phi_k \sum_{i=1}^N h_{i,k+1} \tilde{F}_i(\theta_k + \gamma_k \Phi_k \sum_{j=1}^N \left(\frac{h_{j,k}}{\sigma_h^2} + n_{j,k}\right)) \middle| \mathcal{H}_k\right] \\ &\stackrel{(b)}{=} \mathbb{E}\left[\Phi_k \left( \sum_{i=1}^N h_{i,k+1} \tilde{F}_i(\theta_k) \right. \right. \\ & \quad \left. \left. + \gamma_k \sum_{i=1}^N h_{i,k+1} \sum_{j=1}^N \left(\frac{h_{j,k}}{\sigma_h^2} + n_{j,k}\right) \Phi_k^T \nabla \tilde{F}_i(\theta_k) \right. \right. \\ & \quad \left. \left. + \gamma_k^2 \sum_{i=1}^N h_{i,k+1} \left(\sum_{j=1}^N \frac{h_{j,k}}{\sigma_h^2} + n_{j,k}\right)^2 \Phi_k^T \nabla^2 \tilde{F}_i(\theta_k) \Phi_k \right) \middle| \mathcal{H}_k\right] \\ &\stackrel{(c)}{=} \mathbb{E}\left[\Phi_k \left( \frac{\gamma_k}{\sigma_h^2} \sum_{i=1}^N h_{i,k+1} h_{i,k} \Phi_k^T \nabla \tilde{F}_i(\theta_k) + \right. \right. \\ & \quad \left. \left. + \gamma_k^2 \sum_{i=1}^N h_{i,k+1} \left(\sum_{j=1}^N \frac{h_{j,k}}{\sigma_h^2} + n_{j,k}\right)^2 \Phi_k^T \nabla^2 \tilde{F}_i(\theta_k) \Phi_k \right) \middle| \mathcal{H}_k\right] \\ &= \frac{\gamma_k}{\sigma_h^2} \sum_{i=1}^N \mathbb{E}\left[h_{i,k+1} h_{i,k} \middle| \mathcal{H}_k\right] \mathbb{E}\left[\Phi_k \Phi_k^T \middle| \mathcal{H}_k\right] \nabla \tilde{F}_i(\theta_k) + \\ & \quad \gamma_k^2 \sum_{i=1}^N \mathbb{E}\left[h_{i,k+1} \left(\sum_{j=1}^N \frac{h_{j,k}}{\sigma_h^2} + n_{j,k}\right)^2 \Phi_k^T \nabla^2 \tilde{F}_i(\theta_k) \Phi_k \middle| \mathcal{H}_k\right] \end{aligned}$$

$$\begin{aligned}
& \stackrel{(d)}{=} \gamma_k \alpha_2 \frac{K_{hh}}{\sigma_h^4} \sum_{i=1}^N \nabla F_i(\theta_k) + \\
& \gamma_k^2 \sum_{i=1}^N \mathbb{E} \left[ h_{i,k+1} \left( \sum_{j=1}^N \frac{h_{j,k}}{\sigma_h^2} + n_{j,k} \right)^2 \Phi_k \Phi_k^T \nabla^2 \tilde{F}_i(\check{\theta}_k) \Phi_k \middle| \mathcal{H}_k \right] \\
& \stackrel{(e)}{=} c_1 \gamma_k (\nabla F(\theta_k) + b_k), \\
& \quad (9)
\end{aligned}$$

where (a) is by the definition in (2) and due to Assumption 1, (b) is by Taylor expansion and mean-value theorem and considering  $\check{\theta}_k$  between  $\theta_k$  and  $\theta_k + \gamma_k \Phi_k \sum_{j=1}^N \left( \frac{h_{j,k}}{\sigma_h^2} + n_{j,k} \right)$ . (c) is since  $\mathbb{E}[h_{i,k+1}] = 0$  for the first element and  $\mathbb{E}[h_{i,k+1} h_{j,k}] = 0$  when  $i \neq j$  and the independence of noise for the second element. (d) is due to Assumption 2. In (e), we let  $c_1 = \alpha_2 \frac{K_{hh}}{\sigma_h^4}$  and the bias  $b_k = \gamma_k \frac{\sigma_h^2}{\alpha_2 K_{hh}} \sum_{i=1}^N \mathbb{E} \left[ h_{i,k+1} \left( \sum_{j=1}^N \frac{h_{j,k}}{\sigma_h^2} + n_{j,k} \right)^2 \Phi_k \Phi_k^T \nabla^2 \tilde{F}_i(\check{\theta}_k) \Phi_k \middle| \mathcal{H}_k \right]$ .

### B. Proof of Lemma 2: Expected Norm Squared of the Estimated Gradient

To bound the norm squared of the one-point gradient estimate, we start by letting  $\theta'_k = \theta_k + \gamma_k \Phi_k \sum_{j=1}^N \left( \frac{h_{j,k}}{\sigma_h^2} + n_{j,k} \right)$

$$\begin{aligned}
& \mathbb{E}[\|g_k\|^2 | \mathcal{H}_k] \\
& = \mathbb{E} \left[ \|\Phi_k\|^2 \left( \sum_{i=1}^N h_{i,k+1} \tilde{f}_i(\theta'_k, S_{i,k+1}) + n_{i,k+1} \right)^2 \middle| \mathcal{H}_k \right] \\
& \stackrel{(a)}{\leq} \alpha_3^2 N \sum_{i=1}^N \mathbb{E} \left[ \left( h_{i,k+1} \tilde{f}_i(\theta'_k, S_{i,k+1}) + n_{i,k+1} \right)^2 \middle| \mathcal{H}_k \right] \\
& \stackrel{(b)}{=} \alpha_3^2 N \sum_{i=1}^N \mathbb{E} \left[ h_{i,k+1}^2 \tilde{f}_i^2(\theta'_k, S_{i,k+1}) + n_{i,k+1}^2 \middle| \mathcal{H}_k \right] \\
& \stackrel{(c)}{\leq} \alpha_3^2 N \sum_{i=1}^N \mathbb{E} \left[ \frac{h_{i,k+1}^2}{\sigma_h^4} \left( \|f_i(0, S_{i,k+1})\| + L_{S_{i,k+1}} \|\theta'_k\| \right)^2 \middle| \mathcal{H}_k \right] \\
& \quad + N^2 \alpha_3^2 \sigma_n^2 \\
& \leq \alpha_3^2 N \sum_{i=1}^N \mathbb{E} \left[ \frac{h_{i,k+1}^2}{\sigma_h^4} \left( \|f_i(0, S_{i,k+1})\| + L_{S_{i,k+1}} \|\theta_k\| \right. \right. \\
& \quad \left. \left. + L_{S_{i,k+1}} \gamma_k \|\Phi_k\| \left| \sum_{j=1}^N \frac{h_{j,k}}{\sigma_h^2} + n_{j,k} \right| \right)^2 \middle| \mathcal{H}_k \right] + N^2 \alpha_3^2 \sigma_n^2 \\
& \stackrel{(d)}{\leq} 3 \alpha_3^2 N \sum_{i=1}^N \mathbb{E} \left[ \frac{h_{i,k+1}^2}{\sigma_h^4} \left( \|f_i(0, S_{i,k+1})\|^2 + L_{S_{i,k+1}}^2 \|\theta_k\|^2 \right. \right. \\
& \quad \left. \left. + \alpha_3^2 L_{S_{i,k+1}}^2 \gamma_k^2 \left( \sum_{j=1}^N \frac{h_{j,k}}{\sigma_h^2} + n_{j,k} \right)^2 \right) \middle| \mathcal{H}_k \right] + N^2 \alpha_3^2 \sigma_n^2 \\
& \stackrel{(e)}{\leq} \frac{3N^2 \alpha_3^2}{\sigma_h^2} \left( \mu_S + L_S \|\theta_k\|^2 \right) + 3N \alpha_3^4 L_S \gamma_k^2 \sum_{i=1}^N \mathbb{E} \left[ \frac{h_{i,k+1}^2}{\sigma_h^4} \times \right. \\
& \quad \left. \left( \sum_{j \neq i} \frac{h_{j,k}^2}{\sigma_h^4} + \frac{h_{i,k}^2}{\sigma_h^4} + n_{j,k}^2 + 2 \sum_{j < l} \frac{h_{j,k} h_{l,k}}{\sigma_h^4} \right) \middle| \mathcal{H}_k \right] + N^2 \alpha_3^2 \sigma_n^2
\end{aligned}$$

$$\begin{aligned}
& \stackrel{(f)}{=} \frac{3N^2 \alpha_3^2}{\sigma_h^2} \left( \mu_S + L_S \|\theta_k\|^2 \right) \\
& \quad + 3N^2 \alpha_3^4 L_S \gamma_k^2 \left( \frac{(N-1)\sigma_h^4}{\sigma_h^8} + \frac{\sigma_h^4 + 2K_{hh}^2}{\sigma_h^8} + \frac{N\sigma_n^2}{\sigma_h^2} + 0 \right) \\
& \quad + N^2 \alpha_3^2 \sigma_n^2 \\
& := c_2, \\
& \quad (10)
\end{aligned}$$

where (a) is by Assumption 2 and Cauchy-Schwartz ( $\sum_{j=1}^N 1 \cdot a_i^2 \leq (\sum_{j=1}^N a_i^2) \cdot (\sum_{j=1}^N 1^2) = N(\sum_{j=1}^N a_i^2)$ , for real  $a_i$ ). (b) is due to the independence of noise, (c) is by Assumption 3, and (d) is again by Cauchy-Schwartz. In (e), we let  $\mu_S = \max_i \mathbb{E}[\|f_i(0, S_{i,k+1})\|^2 | \mathcal{H}_k]$  and  $L_S = \max_i \mathbb{E}[L_{S_{i,k+1}}^2 | \mathcal{H}_k]$ . (f) is due to the *normally-distributed* channel random variables,  $\mathbb{E}[h_{i,k+1}^2 \sum_{j \neq i} h_{j,k}^2] = (N-1)\sigma_h^4$ ,  $\mathbb{E}[h_{i,k+1}^2 h_{i,k}^2 | \mathcal{H}_k] = \sigma_h^4 + 2K_{hh}^2$ , and  $\mathbb{E}[h_{i,k+1}^2 \sum_{j < l} h_{j,k} h_{l,k}]$  is equal to zero as one of  $h_{j,k}$  and  $h_{l,k}$  will always be independent of the other terms in the product and has a mean equal to zero.

### C. Proof of Lemma 4: Norm of the Bias

Considering the form of the bias in (9), by Assumptions 1, 2 and 4,

$$\begin{aligned}
& \|b_k\| \\
& \stackrel{(a)}{\leq} \gamma_k \frac{\sigma_h^2}{\alpha_2 K_{hh}} \sum_{i=1}^N \mathbb{E} \left[ 2N \left| h_{i,k+1} \sum_{j=1}^N \left( \frac{h_{j,k}^2}{\sigma_h^4} + n_{j,k}^2 \right) \right| \times \right. \\
& \quad \left. \|\Phi_k\| \|\Phi_k^T\| \|\nabla^2 \tilde{F}_i(\check{\theta}_k)\| \|\Phi_k\| \middle| \mathcal{H}_k \right] \\
& \leq 2\gamma_k \frac{N\alpha_1\alpha_3^3\sigma_h^2}{\alpha_2 K_{hh}} \sum_{i=1}^N \mathbb{E} \left[ \left| h_{i,k+1} \sum_{j=1}^N \left( \frac{h_{j,k}^2}{\sigma_h^4} + n_{j,k}^2 \right) \right| \middle| \mathcal{H}_k \right] \\
& \stackrel{(b)}{\leq} 2\gamma_k \frac{N\alpha_1\alpha_3^3\sigma_h^2}{\alpha_2 K_{hh}} \sum_{i=1}^N \left[ \sigma_h \sqrt{\frac{2}{\pi}} \left( 2K_{hh} + \sqrt{\sigma_h^4 - K_{hh}^2} \right) \right. \\
& \quad \left. + (N-1)\sigma_h^3 \sqrt{\frac{2}{\pi}} + N \sqrt{\frac{2}{\pi}} \sigma_h \sigma_n^2 \right] \\
& = 2\gamma_k \frac{N^2\alpha_1\alpha_3^3\sigma_h^3}{\alpha_2 K_{hh}} \sqrt{\frac{2}{\pi}} \times \\
& \quad \left[ \left( 2K_{hh} + \sqrt{\sigma_h^4 - K_{hh}^2} \right) + (N-1)\sigma_h^2 + N\sigma_n^2 \right] \\
& \stackrel{(c)}{=} c_3 \gamma_k,
\end{aligned}$$

where (a) is due to Jensen's inequality and Cauchy-Schwartz, (b) is by using the half-normal distribution for normal random variables in absolute value explained in the following paragraph, and in (c),  $c_3 = 2 \frac{N^2\alpha_1\alpha_3^3\sigma_h^3}{\alpha_2 K_{hh}} \sqrt{\frac{2}{\pi}} \left[ \left( 2K_{hh} + \sqrt{\sigma_h^4 - K_{hh}^2} \right) + (N-1)\sigma_h^2 + N\sigma_n^2 \right]$ .

Let  $X$  and  $Y$  be two variables representing time-correlated channel realizations at times  $k$  and  $k'$  respectively. Assume they follow the  $\mathcal{N}(0, \sigma)$  distribution and they have a correlation coefficient  $\varrho$ . Then, we can write  $Y = \varrho X + \sqrt{1 - \varrho^2} Z$ , where  $Z$  is independent of  $X$  and following the same distribution  $\mathcal{N}(0, \sigma)$ . Then,  $\mathbb{E}[|YX^2|] \leq \mathbb{E}[\varrho|X^3| + \sqrt{1 - \varrho^2}|ZX^2|] =$

$2\varrho\sqrt{\frac{2}{\pi}}\sigma^3 + \sqrt{1-\varrho^2}\sqrt{\frac{2}{\pi}}\sigma \times \sigma^2 = (2\varrho + \sqrt{1-\varrho^2})\sqrt{\frac{2}{\pi}}\sigma^3$ . If we substitute  $\sigma = \sigma_h$  and  $\varrho = \frac{K_{hh}}{\sigma_h^2}$ , we obtain the previous inequality (b).

## APPENDIX C 1P-ZOFL ALGORITHM CONVERGENCE

### A. Stochastic Noise

To prove Lemma 5, we begin by demonstrating that the sequence  $\{\sum_{k=K}^{K'} \alpha_k e_k\}_{K' \geq K}$  is a martingale. To do so, we have to prove that for all  $K' \geq K$ ,  $X_{K'} = \sum_{k=K}^{K'} \alpha_k e_k$  satisfies the following two conditions:

$$(i) \mathbb{E}[X_{K'+1}|X_{K'}] = X_{K'}$$

$$(ii) \mathbb{E}[\|X_{K'}\|^2] < \infty$$

We know that  $\mathbb{E}[e_k] = \mathbb{E}[g_k - \mathbb{E}[g_k|\mathcal{H}_k]] = \mathbb{E}_{\mathcal{H}_k}[\mathbb{E}[g_k - \mathbb{E}[g_k|\mathcal{H}_k]]|\mathcal{H}_k] = 0$  by the law of total expectation. Hence,  $\mathbb{E}[X_{K'+1}|X_{K'}] = \mathbb{E}[\alpha_{K'+1}e_{K'+1} + \sum_{k=K}^{K'} \alpha_k e_k | \sum_{k=K}^{K'} \alpha_k e_k] = 0 + \sum_{k=K}^{K'} \alpha_k e_k = X_{K'}$ .

In addition,  $e_k$  and  $e_{k'}$  are uncorrelated for any  $k \neq k'$  since (assuming  $k > k'$ )  $\mathbb{E}[e_k^T e_{k'}] = \mathbb{E}[\mathbb{E}[e_k^T e_{k'}|\mathcal{H}_k]] = \mathbb{E}[e_k^T \mathbb{E}[e_{k'}|\mathcal{H}_k]] = 0$ . Thus,

$$\begin{aligned} \mathbb{E}(\|\sum_{k=K}^{K'} \alpha_k e_k\|^2) &= \mathbb{E}(\sum_{k=K}^{K'} \sum_{k'=K}^{K'} \alpha_k \alpha_{k'} \langle e_k, e_{k'} \rangle) \\ &\stackrel{(a)}{=} \mathbb{E}(\sum_{k=K}^{K'} \|\alpha_k e_k\|^2) \\ &\leq \sum_{k=K}^{\infty} \mathbb{E}(\alpha_k^2 \|g_k - \mathbb{E}[g_k|\mathcal{H}_k]\|^2) \\ &= \sum_{k=K}^{\infty} \alpha_k^2 \mathbb{E}(\|g_k\|^2) - \mathbb{E}_{\mathcal{H}_k}(\|\mathbb{E}[g_k|\mathcal{H}_k]\|^2) \\ &\leq \sum_{k=K}^{\infty} \alpha_k^2 \mathbb{E}(\|g_k\|^2) \stackrel{(b)}{\leq} c_2 \sum_{k=K}^{\infty} \alpha_k^2 \gamma_k^2 \stackrel{(c)}{<} \infty, \end{aligned} \quad (12)$$

where (a) is due to the uncorrelatedness  $\mathbb{E}[\langle e_k, e_{k'} \rangle] = 0$ , (b) is by Lemma 2, and (c) is by Assumption 5. Therefore, both (i) and (ii) are satisfied and we can say that  $\{\sum_{k=K}^{K'} \alpha_k e_k\}_{K' \geq K}$  is a martingale. This permits us to use Doob's martingale inequality [38]:

For any constant  $\nu > 0$ ,

$$\begin{aligned} \mathbb{P}(\sup_{K' \geq K} \|\sum_{k=K}^{K'} \alpha_k e_k\| \geq \nu) &\leq \frac{1}{\nu^2} \mathbb{E}(\|\sum_{k=K}^{K'} \alpha_k e_k\|^2) \\ &\stackrel{(a)}{\leq} \frac{c_2}{\nu^2} \sum_{k=K}^{\infty} \alpha_k^2 \gamma_k^2, \end{aligned} \quad (13)$$

where (a) is following the exact same steps as (12).

Since  $c_2$  is a bounded constant and  $\lim_{K \rightarrow \infty} \sum_{k=K}^{\infty} \alpha_k^2 \gamma_k^2 = 0$  by Assumption 5, we get  $\lim_{K \rightarrow \infty} \frac{c_2}{\nu^2} \sum_{k=K}^{\infty} \alpha_k^2 \gamma_k^2 = 0$  for any bounded constant  $\nu$ . Hence, the probability that  $\|\sum_{k=K}^{K'} \alpha_k e_k\| \geq \nu$  also vanishes as  $K \rightarrow \infty$ , which concludes the proof.

### B. Proof of Theorem 1: Convergence Analysis

By the  $L$ -smoothness assumption and the algorithm update step  $\theta_{k+1} = \theta_k - \alpha_k g_k$ , we have

$$\begin{aligned} &F(\theta_{k+1}) \\ &\leq F(\theta_k) - \alpha_k \langle \nabla F(\theta_k), g_k \rangle + \frac{\alpha_k^2 L}{2} \|g_k\|^2 \\ &= F(\theta_k) - \alpha_k \langle \nabla F(\theta_k), e_k + \mathbb{E}[g_k|\mathcal{H}_k] \rangle + \frac{\alpha_k^2 L}{2} \|g_k\|^2 \\ &= F(\theta_k) - \alpha_k \langle \nabla F(\theta_k), e_k \rangle - c_1 \alpha_k \gamma_k \|\nabla F(\theta_k)\|^2 \\ &\quad - c_1 \alpha_k \gamma_k \langle \nabla F(\theta_k), b_k \rangle + \frac{\alpha_k^2 L}{2} \|g_k\|^2 \\ &\stackrel{(a)}{\leq} F(\theta_k) - \alpha_k \langle \nabla F(\theta_k), e_k \rangle - c_1 \alpha_k \gamma_k \|\nabla F(\theta_k)\|^2 \\ &\quad + \frac{c_1 \alpha_k \gamma_k}{2} \|\nabla F(\theta_k)\|^2 + \frac{c_1 \alpha_k \gamma_k}{2} \|b_k\|^2 + \frac{\alpha_k^2 L}{2} \|g_k\|^2 \\ &= F(\theta_k) - \alpha_k \langle \nabla F(\theta_k), e_k \rangle - \frac{c_1 \alpha_k \gamma_k}{2} \|\nabla F(\theta_k)\|^2 \\ &\quad + \frac{c_1 \alpha_k \gamma_k}{2} \|b_k\|^2 + \frac{\alpha_k^2 L}{2} \|g_k\|^2 \end{aligned} \quad (14)$$

where (a) is by  $-\langle a, b \rangle \leq \frac{1}{2} \|a\|^2 + \frac{1}{2} \|b\|^2$ .

By taking the telescoping sum, we get

$$\begin{aligned} F(\theta^*) &\leq F(\theta_{K+1}) \leq F(\theta_0) - \frac{c_1}{2} \sum_{k=0}^K \alpha_k \gamma_k \|\nabla F(\theta_k)\|^2 \\ &\quad - \sum_{k=0}^K \alpha_k \langle \nabla F(\theta_k), e_k \rangle \\ &\quad + \frac{c_1}{2} \sum_{k=0}^K \alpha_k \gamma_k \|b_k\|^2 + \frac{c_2 L}{2} \sum_{k=0}^K \alpha_k^2 \|g_k\|^2 \end{aligned} \quad (15)$$

Hence,

$$\begin{aligned} \sum_{k=0}^K \alpha_k \gamma_k \|\nabla F(\theta_k)\|^2 &\leq \frac{2}{c_1} (F(\theta_0) - F(\theta^*)) \\ &\quad - \frac{2}{c_1} \sum_{k=0}^K \alpha_k \langle \nabla F(\theta_k), e_k \rangle \\ &\quad + \sum_{k=0}^K \alpha_k \gamma_k \|b_k\|^2 + \frac{c_2 L}{c_1} \sum_{k=0}^K \alpha_k^2 \|g_k\|^2 \end{aligned} \quad (16)$$

By Assumption 3,  $\|\nabla F(\theta_k)\|$  is bounded for any  $\theta_k \in \mathbb{R}^d$  and by taking the summation in (13) between 0 and  $\infty$ , we have

$$\lim_{K \rightarrow \infty} \left\| \sum_{k=0}^K \alpha_k \langle \nabla F(\theta_k), e_k \rangle \right\| < \infty. \quad (17)$$

From Lemma 4, we know that  $\|b_k\|^2 \sim \gamma_k^2$ . Hence, by Assumption 5,  $\lim_{K \rightarrow \infty} \sum_{k=0}^K \alpha_k \gamma_k^3 < \infty$ .

From Lemma 2 and by looking closely at the use of the Lipschitz continuity property in (10), we can say

$\|g_k\|^2 \leq c$  for some  $c > 0$ . Thus, again by Assumption 5,  $\lim_{K \rightarrow \infty} \sum_{k=0}^K \alpha_k^2 < \infty$ . We conclude that

$$\lim_{K \rightarrow \infty} \sum_{k=0}^K \alpha_k \gamma_k \|\nabla F(\theta_k)\|^2 < \infty. \quad (18)$$

Moreover, since the series  $\sum_k \alpha_k \gamma_k$  diverges by Assumption 5, we have  $\lim_{k \rightarrow \infty} \inf \|\nabla F(\theta_k)\| = 0$ .

To prove that  $\lim_{k \rightarrow \infty} \|\nabla F(\theta_k)\| = 0$ , we consider the hypothesis H)  $\lim_{k \rightarrow \infty} \sup \|\nabla F(\theta_k)\| \geq \rho$  for an arbitrary  $\rho > 0$ .

Assume (H) to be true. Then, we can always find an arbitrary subsequence  $(\|\nabla F(\theta_{k_l})\|)_{l \in \mathbb{N}}$  of  $\|\nabla F(\theta_k)\|$ , such that  $\|\nabla F(\theta_{k_l})\| \geq \rho - \varepsilon$ ,  $\forall l$ , for  $\rho - \varepsilon > 0$  and  $\varepsilon > 0$ .

Then, by the  $L$ -smoothness property and applying the descent step of the algorithm,

$$\begin{aligned} \|\nabla F(\theta_{k_l+1})\| &\geq \|\nabla F(\theta_{k_l})\| - \|\nabla F(\theta_{k_l+1}) - \nabla F(\theta_{k_l})\| \\ &\geq \rho - \varepsilon - L\|\theta_{k_l+1} - \theta_{k_l}\| \\ &= \rho - \varepsilon - L\alpha_{k_l} \|g_{k_l}\| \\ &\geq \rho - \varepsilon - L\sqrt{c}\alpha_{k_l}, \end{aligned} \quad (19)$$

Since  $k_l \rightarrow \infty$  as  $l \rightarrow \infty$ , we can always find a subsequence of  $(k_{l_p})_{p \in \mathbb{N}}$  such that  $k_{l_{p+1}} - k_{l_p} > 1$ . As  $\alpha_{k_l}$  is vanishing, we consider  $(k_l)_{l \in \mathbb{N}}$  starting from  $\alpha_{k_l} < \frac{\rho - \varepsilon}{L\sqrt{c}}$ . Thus,

$$\begin{aligned} &\sum_{k=0}^{\infty} \alpha_{k+1} \gamma_{k+1} \|\nabla F(\theta_{k+1})\|^2 \\ &\geq (\rho - \varepsilon)^2 \sum_{k=0}^{\infty} \alpha_{k+1} \gamma_{k+1} - 2(\rho - \varepsilon)L\sqrt{c} \sum_{k=0}^{\infty} \alpha_{k+1} \gamma_{k+1} \alpha_k \\ &\quad + L^2 c \sum_{k=0}^{\infty} \alpha_{k+1} \gamma_{k+1} \alpha_k^2 \\ &= +\infty, \end{aligned} \quad (20)$$

as the first series diverges, and the second and the third converge by Assumption 5. This implies that the series  $\sum_k \alpha_k \gamma_k \|\nabla F(\theta_k)\|^2$  diverges. This is a contradiction as this series converges almost surely by (18). Therefore, hypothesis (H) cannot be true and  $\|\nabla F(\theta_k)\|$  converges to zero almost surely.

### C. Proof of Theorem 2: Convergence Rate

Starting again from the  $L$ -smoothness in Lemma 3 and the algorithm update step  $\theta_{k+1} = \theta_k - \alpha_k g_k$ , we have

$$F(\theta_{k+1}) \leq F(\theta_k) - \alpha_k \langle \nabla F(\theta_k), g_k \rangle + \frac{\alpha_k^2 L}{2} \|g_k\|^2. \quad (21)$$

Taking the conditional expectation given  $\mathcal{H}_k$ ,

$$\begin{aligned} &F(\theta_{k+1}) \\ &\leq F(\theta_k) - c_1 \alpha_k \gamma_k \langle \nabla F(\theta_k), \nabla F(\theta_k) + b_k \rangle + \frac{\alpha_k^2 L c_2}{2} \\ &= F(\theta_k) - c_1 \alpha_k \gamma_k \|\nabla F(\theta_k)\|^2 - c_1 \alpha_k \gamma_k \langle \nabla F(\theta_k), b_k \rangle \\ &\quad + \frac{\alpha_k^2 L c_2}{2} \end{aligned}$$

$$\begin{aligned} &\stackrel{(a)}{\leq} F(\theta_k) - c_1 \alpha_k \gamma_k \|\nabla F(\theta_k)\|^2 + \frac{c_1 \alpha_k \gamma_k}{2} \|\nabla F(\theta_k)\|^2 \\ &\quad + \frac{c_1 \alpha_k \gamma_k}{2} \|b_k\|^2 + \frac{\alpha_k^2 L c_2}{2} \\ &= F(\theta_k) - \frac{c_1 \alpha_k \gamma_k}{2} \|\nabla F(\theta_k)\|^2 + \frac{c_1 \alpha_k \gamma_k}{2} \|b_k\|^2 + \frac{\alpha_k^2 L c_2}{2} \end{aligned} \quad (22)$$

where (a) is by  $-\langle a, b \rangle \leq \frac{1}{2} \|a\|^2 + \frac{1}{2} \|b\|^2$

By considering a large value  $K > 0$  and taking the telescoping sum of (22), we get

$$\begin{aligned} &\mathbb{E}[F(\theta_{K+1}) | \mathcal{H}_K] \\ &\leq F(\theta_0) - \frac{c_1}{2} \sum_{k=0}^K \alpha_k \gamma_k \|\nabla F(\theta_k)\|^2 + \frac{c_1}{2} \sum_{k=0}^K \alpha_k \gamma_k \|b_k\|^2 \\ &\quad + \frac{L c_2}{2} \sum_{k=0}^K \alpha_k^2. \end{aligned} \quad (23)$$

Given the assumption that  $F(\theta^*) = \min_{\theta \in \mathbb{R}^d} F(\theta)$  exists, we know that  $\delta_k = F(\theta_k) - F(\theta^*) \geq 0$ . Then,

$$\begin{aligned} 0 \leq \mathbb{E}[\delta_{K+1} | \mathcal{H}_K] &\leq \delta_0 - \frac{c_1}{2} \sum_{k=0}^K \alpha_k \gamma_k \|\nabla F(\theta_k)\|^2 \\ &\quad + \frac{c_1 c_3}{2} \sum_{k=0}^K \alpha_k \gamma_k^3 + \frac{L c_2}{2} \sum_{k=0}^K \alpha_k^2. \end{aligned} \quad (24)$$

Finally,

$$\sum_k \alpha_k \gamma_k \mathbb{E}[\|\nabla F(\theta_k)\|^2] \leq \frac{2}{c_1 c_3} \delta_0 + \sum_k \alpha_k \gamma_k^3 + \frac{L c_2}{c_1} \sum_k \alpha_k^2 \quad (25)$$

Let  $\alpha_k$  and  $\gamma_k$  have the forms given in Example 2. We know that,  $\forall K > 0$ ,

$$\begin{aligned} \sum_{k=0}^K \alpha_k \gamma_k^3 &= \alpha_0 \gamma_0^3 + \sum_{k=1}^K \alpha_k \gamma_k^3 \\ &\leq \alpha_0 \gamma_0^3 \left(1 + \int_0^K (x+1)^{-v_1-3v_2} dx\right) \\ &\leq \alpha_0 \gamma_0^3 \left(1 + \frac{1}{v_1+3v_2-1}\right) \\ &= \alpha_0 \gamma_0^3 \left(\frac{v_1+3v_2}{v_1+3v_2-1}\right). \end{aligned} \quad (26)$$

Similarly,  $\sum_{k=0}^K \alpha_k^2 \leq \alpha_0^2 \left(\frac{2v_1}{2v_1-1}\right)$ . Next, when further  $0 < v_1 + v_2 < 1$ ,

$$\begin{aligned} \sum_{k=0}^K \alpha_k \gamma_k &\geq \alpha_0 \gamma_0 \int_0^{K+1} (x+1)^{-v_1-v_2} dx \\ &= \frac{\alpha_0 \gamma_0}{(1-v_1-v_2)} \left((K+2)^{1-v_1-v_2} - 1\right). \end{aligned} \quad (27)$$

Thus, making use of inequality (25)

$$\frac{\sum_k \alpha_k \gamma_k \mathbb{E}[\|\nabla F(\theta_k)\|^2]}{\sum_k \alpha_k \gamma_k} \leq \frac{A(1-v_1-v_2)}{(K+2)^{1-v_1-v_2}-1} \quad (28)$$

with  $A = \frac{2}{c_1 \alpha_0 \gamma_0} \delta_0 + c_3^2 \gamma_0^2 \left(\frac{v_1+3v_2}{v_1+3v_2-1}\right) + \frac{L c_2 \alpha_0}{c_1 \gamma_0} \left(\frac{2v_1}{2v_1-1}\right)$

## APPENDIX D NON-SYMMETRICAL CHANNELS

Assuming non-symmetrical channels with  $\mathbb{E}[h_{i,k}] = \mu_h$  and  $\sigma_h^2 = \mathbb{E}[h_{i,k}^2] - \mu_h^2$ ,  $\forall i, \forall k$ , the one-point gradient estimate becomes

$$g_k = \Phi_k \sum_{i=1}^N \left[ h_{i,k+1} \tilde{f}_i(\theta_k + \gamma_k \Phi_k, S_{i,k+1}) + n_{i,k+1} \right]. \quad (29)$$

And 1P-ZOFL is updated to Algorithm 2. We then analyze

**Algorithm 2** The 1P-ZOFL algorithm with non-symmetrical channels

**Input:** Initial model  $\theta_0 \in \mathbb{R}^d$ , the initial step-sizes  $\alpha_0$  and  $\gamma_0$ , and the channels' standard deviation  $\sigma_h$

- 1: **for**  $k = 0, 2, 4, \dots$  **do**
- 2: The server broadcasts  $\theta_k + \gamma_k \Phi_k$
- 3: The server receives  $\sum_{i=1}^N h_{i,k+1} \tilde{f}_i(\theta_k + \gamma_k \Phi_k, S_{i,k+1}) + n_{i,k+1}$
- 4: The server multiplies the received scalar sum by  $\Phi_k$  to assemble  $g_k$  in (29)
- 5: The server updates  $\theta_{k+1} = \theta_k - \alpha_k g_k$
- 6: **end for**

the properties of our modified gradient estimate:

$$\begin{aligned} & \mathbb{E}[g_k | \mathcal{H}_k] \\ &= \mathbb{E}\left[\Phi_k \sum_{i=1}^N \left( h_{i,k+1} \tilde{f}_i(\theta_k + \gamma_k \Phi_k, S_{i,k+1}) + n_{i,k+1} \right) \middle| \mathcal{H}_k\right] \\ &= \mathbb{E}\left[\Phi_k \sum_{i=1}^N \mu_h \tilde{F}_i(\theta_k + \gamma_k \Phi_k) \middle| \mathcal{H}_k\right] \\ &= \mu_h \gamma_k \sum_{i=1}^N \mathbb{E}\left[\Phi_k \Phi_k^T \nabla \tilde{F}_i(\theta_k) + \gamma_k \Phi_k \Phi_k^T \nabla^2 \tilde{F}_i(\check{\theta}_k) \Phi_k \middle| \mathcal{H}_k\right] \\ &= c_1 \gamma_k (\nabla F(\theta_k) + b_k), \end{aligned} \quad (30)$$

with  $c_1 = \frac{\mu_h \alpha_2}{\sigma_h^2}$  and  $b_k = \frac{\gamma_k}{\alpha_2} \mathbb{E}\left[\Phi_k \Phi_k^T \nabla^2 F_i(\check{\theta}_k) \Phi_k \middle| \mathcal{H}_k\right]$ .

Then,  $\|b_k\| \leq \frac{\gamma_k}{\alpha_2} \alpha_3^3 \alpha_1$ , now  $c_3 = \frac{\alpha_3^3 \alpha_1}{\alpha_2}$  and  $\|b_k\| \leq c_3 \gamma_k$ . Let  $\theta'_k = \theta_k + \gamma_k \Phi_k$ ,

$$\begin{aligned} & \mathbb{E}[\|g_k\|^2 | \mathcal{H}_k] \\ &= \mathbb{E}\left[\|\Phi_k\|^2 \left( \sum_{i=1}^N h_{i,k+1} \tilde{f}_i(\theta'_k, S_{i,k+1}) + n_{i,k+1} \right)^2 \middle| \mathcal{H}_k\right] \\ &= \alpha_3^2 N \sum_{i=1}^N \mathbb{E}\left[h_{i,k+1}^2 \tilde{f}_i^2(\theta'_k, S_{i,k+1}) + n_{i,k+1}^2 \middle| \mathcal{H}_k\right] \\ &\leq \alpha_3^2 N \sum_{i=1}^N \mathbb{E}\left[\frac{h_{i,k+1}^2}{\sigma_h^4} \left( \|f_i(0, S_{i,k+1})\| + L_{S_{i,k+1}} \|\theta'_k\| \right)^2 \middle| \mathcal{H}_k\right] \\ &\quad + N^2 \alpha_3^2 \sigma_n^2 \end{aligned}$$

$$\begin{aligned} &\leq 3\alpha_3^2 N \sum_{i=1}^N \mathbb{E}\left[\frac{h_{i,k+1}^2}{\sigma_h^4} \left( \|f_i(0, S_{i,k+1})\|^2 + L_{S_{i,k+1}}^2 \|\theta_k\|^2 \right. \right. \\ &\quad \left. \left. + \alpha_3^2 L_{S_{i,k+1}}^2 \gamma_k^2 \right) \middle| \mathcal{H}_k\right] + N^2 \alpha_3^2 \sigma_n^2 \\ &= \frac{3N^2 \alpha_3^2 (\sigma_h^2 + \mu_h^2)}{\sigma_h^2} \left( \mu_S + L_S \|\theta_k\|^2 + \alpha_3^2 L_S \gamma_k^2 \right) + N^2 \alpha_3^2 \sigma_n^2 \\ &:= c_2. \end{aligned} \quad (31)$$

## APPENDIX E EXPERIMENTAL RESULTS DETAILS

### A. Autoencoder

We compress images from the MNIST dataset using a lossy autoencoder with encoder-decoder architecture. The encoder reduces the input size from 784 to 10 through three linear layers with dimensions 784-512-128-10. The first two layers have ELU activation functions. The decoder reverses this process, going from 10 to 784 through three linear layers (10-128-512-784), with ELU activation in the first two layers and a sigmoid activation in the last layer to ensure output pixel intensities between 0 and 1. Training is done on the MNIST dataset for 10 epochs, using mean squared error loss and the Adam optimizer.

### B. Performance of 1P-ZOFL vs SNR

An important remark is that high SNR is generally needed when we must decode the information in the received signal. In our case, nothing is decoded; there is no channel estimation or gradient extraction from the received signal. Rather, the received signal is fed directly into the learning (the channel is part of the learning). Ultimately, the amount of noise present in the system does not affect our algorithms' convergence: Examining (10) and (11), we see that the noise variance  $\sigma_n^2$  might only increase the norms of the estimate and bias, but if we refer to (14), we find that both terms are multiplied by step sizes, and we can counter the noise effect by decreasing the step sizes' constant parts (i.e., in the terms  $\frac{c_1 \alpha_k \gamma_k}{2} \|b_k\|^2$  and  $\frac{\alpha_k^2 L}{2} \|g_k^{(1P)}\|^2$ ). For the different plots in Fig. 3, we decrease  $\alpha_0$  and  $\gamma_0$  when we increase  $\sigma_n^2$ . However, this change of step sizes generally affects the rate of convergence as they enter in the structure of  $g_k$  and  $b_k$  themselves and as can be seen in (4), smaller  $\alpha_0$  and  $\gamma_0$  increases the first term in the constant part of the upper bound on the convergence rate. Thus, the effect shown on the plots in Fig. 3 is logical given the changes of  $\alpha_0$  and  $\gamma_0$ .